

# Piezoelectric Vibration-Type Tactile Sensor Using Elasticity and Viscosity Change of Structure

Kohei Motoo, Fumihito Arai, and Toshio Fukuda, *Fellow, IEEE*

**Abstract**—We propose a new tactile sensor utilizing piezoelectric vibration. This tactile sensor has a high sensitivity, wide measurement range, pressure resistance, flexibility, and self-sensing function. This tactile sensor comprises two piezoelectric materials. One is used for the vibration of the sensor element and the other is used for the measurement of the change in mechanical impedance induced by an external force. We achieved the wide measurement range by implementing two ideas. One was to apply the external force to the sensor element through an elastic body and the other was to use two or more modes of vibration. Moreover, for the elastic body, it is preferable to use a material whose elasticity and viscosity are easily changed by an external force, such as a gel. In this study, first, this tactile sensor was analyzed, and then its characteristics were derived. The analytical results qualitatively corresponded to the experimental results. Next, a prototype tactile sensor was fabricated and evaluated. The evaluation results showed that this tactile sensor can measure a pressure of 2.5 Pa or less and a pressure of 10 kPa or more and its pressure resistance is 1 MPa or more.

**Index Terms**—Piezoelectric vibration-type sensor, robot hand, self-sensing, tactile sensor.

## I. INTRODUCTION

**A**N EXCELLENT tactile sensor is needed in the fields of robotics, medical treatment, and caring. In particular, in the field of humanoid robot, a tactile sensor that has a tactile sensitivity equal to that of human beings, a wide measurement range, and high durability is needed for artificial skin and a robotic hand.

To achieve dexterous manipulations as human beings do with a robotic hand, a tactile sensor that has a tactile sensitivity equal to that of human beings (tens of Pa) is necessary. Moreover, a tactile sensor that has a wide measurement range (up to hundreds of kPa) is necessary to do heavy lifting in place of human beings. That is, a tactile sensor whose ratio between minimum and maximum measurement value is at least  $10^4$  or more is necessary.

Tactile sensors utilizing a strain gauge [1], electric capacitance [2], conductive rubber [3], and a piezoelectric polymer film [4] have been developed. In general, such tactile sensors have the following disadvantages. When the tactile sensor has a high sensitivity, its reaction to an applied force easily becomes saturated, and when its reaction to an applied force is not easily

Manuscript received June 9, 2006; revised January 1, 2007; accepted January 18, 2007. The associate editor coordinating the review of this paper and approving it for publication was Dr. Andre Bossche.

K. Motoo and T. Fukuda are with the Department of Micro-Nano Systems Engineering, Nagoya University, Furo-cho, Chikusa-ku, Nagoya 464-8603, Japan (e-mail: motoo@robo.mein.nagoya-u.ac.jp; fukuda@mein.nagoya-u.ac.jp).

F. Arai is with the Department of Bioengineering and Robotics, Tohoku University, 6-6-01, Aramaki-Aoba, Aoba-ku, Sendai 980-8579, Japan (e-mail: arai@imech.mech.tohoku.ac.jp).

Digital Object Identifier 10.1109/JSEN.2007.895973

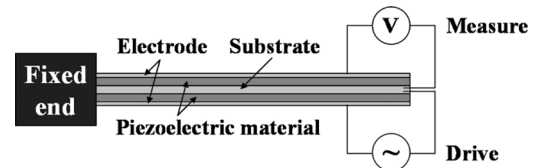


Fig. 1. Piezoelectric vibration-type sensor. The system consists of a substrate, piezoelectric materials, and electrodes.

saturated, the sensitivity of the tactile sensor is lower because it utilizes transformation of its constituent material to detect the force; that is, the measurement range is not sufficient. In particular, the realization of a tactile sensor for a humanoid robot that has both a tactile sensitivity equal to that of human beings and a wide measurement range is difficult. For example, although the tactile sensor which utilizes pressure sensitive and conductive ink films [5] is frequently used for a robotic hand [6], the ratio between minimum and maximum measurement value is around 10. So, it becomes impossible to achieve a balance between lift of heavy object and dexterous manipulation of small and fragile object. On the other hand, a tactile sensor utilizing light has been developed [7], [8]. In general, since a tactile sensor based on this principle requires a charge-coupled device (CCD) camera and image data processing, miniaturization is difficult and the cost is high although a wide measurement range can be realized.

To date, a variety of tactile sensors have been proposed, as described in [9]. Moreover, some research on applying such tactile sensors to a humanoid robot has also been carried out [10]. However, since a tactile sensor that exhibits all of the desired characteristics, including high sensitivity, wide measurement range, high durability, and low cost, has not yet been realized, at present, such tactile sensors are not used for humanoid robots at a practical level. Therefore, in this paper, we propose a new tactile sensor utilizing piezoelectric vibration that has a high sensitivity, wide measurement range, pressure resistance, flexibility, and self-sensing function and is comparatively small and of low cost.

The principle of the piezoelectric vibration-type sensor [11] is now explained with reference to Fig. 1. This sensor has two electrodes. One is for driving and the other is for measurement.

- 1) The driving electrode is supplied with an alternating current, and the sensor is resonated due to the inverse piezoelectric effect.
- 2) A voltage is generated by the piezoelectric effect in the measurement electrode.
- 3) When an external force is applied to the sensor, the mechanical impedance changes, and the voltage of the measurement electrode changes.
- 4) The external force is measured on the basis of this voltage change.

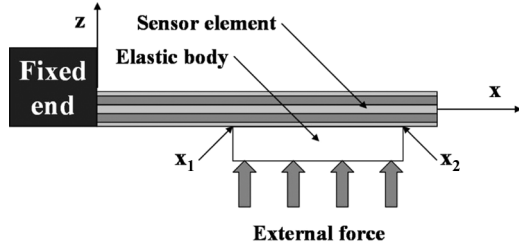


Fig. 2. Experimental model of tactile sensor. The elastic body is arranged from  $x_1$  to  $x_2$ . An external force is applied to the sensor element through the elastic body.

It should be noted that the sensor can be used not only in the fixed condition shown in Fig. 1, but also in various fixed conditions, such as both ends being supported or both ends being fixed in place, and the pressure resistance is adjusted by proper selection of the substrate.

Since piezoelectric vibration-type sensors have a high sensitivity and high pressure resistance, they have been used for scanning force microscopy (SFM) [12] and as a touch sensor for micromanipulation [13], [14]. However, since such sensors easily become saturated with a large change in mechanical impedance, their measurement range is extremely narrow even though they have a high sensitivity for a small change in mechanical impedance. Therefore, their use as a tactile sensor is limited, for example, in application to a humanoid robot, although their use as a touch sensor is possible.

Therefore, we realize a piezoelectric vibration-type sensor as a tactile sensor by using two ideas. One is to apply an external force to the sensor through its elastic body. As a result, the change in mechanical impedance induced by the external force occurs gently, and the measurement range of the sensor is widened. In addition, the change in mechanical impedance becomes larger when a material whose elasticity and viscosity are easily changed by an external force, such as a gel, is used as the elastic body, and the measurement range becomes wider as a result (for instance, the nonlinear characteristic of the gel is described in [15] in detail). Moreover, the surface is flexible when such a material is used. The other is to use two or more modes of vibration. As a result, expansion of the measurement range and adjustment of sensitivity become possible.

Since this tactile sensor has both sensor and actuator functions, self-sensing is possible. Thus, when this tactile sensor is applied to a humanoid robot, improvement of operational safety is expected because the robot itself can recognize the breakdown of the tactile sensor by using this self-sensing function.

In this study, first, this tactile sensor is analyzed and its characteristics are derived. Next, a prototype is produced, and the validity of the analytical results is investigated. Finally, the pressure resistance of this tactile sensor is evaluated.

## II. ANALYSIS

The tactile sensor is now analyzed, and the output voltage induced by the piezoelectric effect is derived. The experimental model is shown in Fig. 2. The elastic body is arranged from  $x_1$  to  $x_2$ . An external force is applied to the sensor element through the elastic body. The analytical model is shown in Fig. 3. The elastic body is assumed to be composed of a material whose elasticity and viscosity are easily changed by an external force,

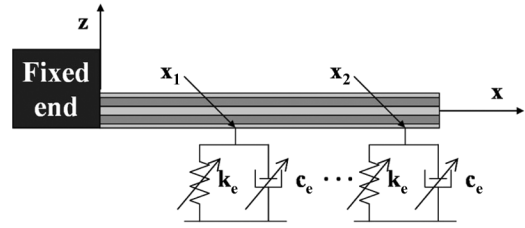


Fig. 3. Analytical model of tactile sensor. The elasticity and viscosity are expressed as  $k_e$  and  $c_e$ , respectively.

such as a gel. The elasticity and viscosity are expressed as  $k_e$  and  $c_e$ , respectively. First, the displacement caused by the inverse piezoelectric effect is derived by modal analysis. The displacement  $z$  is expressed as follows by a summation of the mode function  $Z_n$  and time function  $\xi_n$

$$z = \sum_{n=1}^{\infty} Z_n \xi_n \quad (1)$$

where

$$\xi_n \equiv B e^{j\omega_n t} \quad (2)$$

$B$  is constant, and  $\omega_n$  is the natural angular frequency of the sensor element. When the sensor resonates at a certain mode of vibration, (1) can be reduced to the following because the displacement caused by other modes of vibration is very small:

$$z \equiv z_n = Z_n \xi_n. \quad (3)$$

The motion equation of this tactile sensor is expressed as

$$\int_0^L \rho A Z_n^2 dx \ddot{\xi}_n + \int_0^L c Z_n^2 dx \dot{\xi}_n + \omega_n^2 \int_0^L \rho A Z_n^2 dx \xi_n = Q_n \quad (4)$$

where  $L$  is the length of the sensor element,  $\rho$  is the density of the sensor element,  $A$  is the cross-sectional area of the sensor element,  $c$  is the viscous damping coefficient of the sensor element, and  $Q_n$  is the generalized force. The generalized force is expressed as

$$Q_n = \int_0^L Z_n \frac{\partial M_x}{\partial x} dx - \int_{x_1}^{x_2} b k_e z_n Z_n dx - \int_{x_1}^{x_2} b c_e \dot{z}_n Z_n dx \quad (5)$$

where  $M_x$  is the bending moment due to the inverse piezoelectric effect, and  $b$  is the width of the sensor element. The fundamental piezoelectric equation is expressed as [16], [17]

$$S_x = \frac{1}{Y_p} \sigma_x + d_{31} E_z \quad (6)$$

where  $S_x$  is the strain,  $Y_p$  is the Young's modulus of the piezoelectric material,  $\sigma_x$  is the stress,  $d_{31}$  is the piezoelectric constant, and  $E_z$  is the electric field. From (6), the bending moment is expressed as

$$M_x = \int_{t_s}^{t_s+t_p} b \sigma_x z dz [u(x) - u(x-L)] = \frac{b Y_p d_{31} V (2t_s + t_p) [u(x) - u(x-L)] e^{j\omega_n t}}{2} \quad (7)$$

where  $t_s$  is half the thickness of the substrate,  $t_p$  is the thickness of the piezoelectric material,  $u(x)$  is a unit step function, and  $V$  is the input voltage. When (2), (3), and (7) are substituted in (5), the generalized force is expressed as

$$Q_n = \frac{b}{2} \left\{ Y_p d_{31} V (2t_s + t_p) \int_0^L Z_n [\delta(x) - \delta(x-L)] dx - 2B(k_e + jc_e \omega_n) A_x \right\} e^{j\omega_n t} \quad (8)$$

where

$$A_x \equiv \int_{x_1}^{x_2} Z_n^2 dx \quad (9)$$

$\delta(x)$  is the delta function. When (2) and (8) are substituted in (4), constant  $B$  is expressed as

$$B = \frac{bY_p d_{31} V (2t_s + t_p) \int_0^L Z_n [\delta(x) - \delta(x-L)] dx}{2[bk_e A_x + j\omega_n (bc_e A_x + cA_L)]} \quad (10)$$

where

$$A_L \equiv \int_0^L Z_n^2 dx. \quad (11)$$

When (2) and (10) are substituted in (3), the displacement is expressed, as shown in (12) at the bottom of the page, where

$$\tan \phi = \frac{\omega_n (bc_e A_x + cA_L)}{bk_e A_x}. \quad (13)$$

Next, the output voltage induced by the piezoelectric effect is derived. The output voltage  $V_s$  is expressed as

$$V_s = \frac{Q}{C} = \frac{\int_S D_z dS}{C} \quad (14)$$

where  $Q$  is the quantity of electric charge,  $C$  is the electric capacitance,  $S$  is the surface area, and  $D_z$  is the electric displacement. The fundamental piezoelectric equation is expressed as [16], [17]

$$D_z = d_{31} \sigma_x + \varepsilon_3^T E_z \quad (15)$$

where  $\varepsilon_3$  is the permittivity of the piezoelectric material. From (15), the electric displacement is expressed as [16]

$$D_z = -\frac{d_{31} Y_p (2t_s + t_p)}{2} \frac{\partial^2 z_n}{\partial x^2}. \quad (16)$$

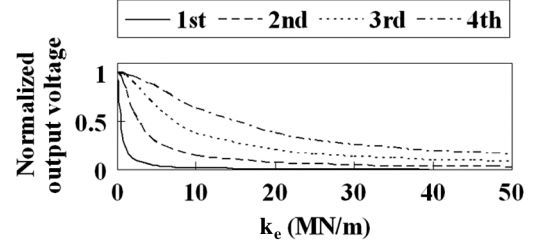


Fig. 4. Simulation results. Relationship between normalized output voltage and elasticity ( $x_1 = 0$  mm,  $x_2 = 7.5$  mm).

When (12) and (16) are substituted in (14), the output voltage is expressed, as shown in (17) at the bottom of the page.

A simulation was carried out to investigate the characteristics of this tactile sensor with respect to the mode of vibration and the arrangement of the elastic body. To clarify the change in the characteristics caused by a change in the mode of vibration, (17) was normalized as

$$V_1 \equiv \frac{V_s}{V_0} \quad (18)$$

$$= \frac{\omega_n c A_L}{\sqrt{(bk_e A_x)^2 + \omega_n^2 (bc_e A_x + cA_L)^2}} \quad (19)$$

where  $V_0$  is the output voltage when the sensor element is not in contact with the elastic body ( $k_e = 0$ ,  $c_e = 0$ ). The relationships between output voltage  $V_1$  and elasticity  $k_e$  and between output voltage  $V_1$  and viscosity  $c_e$  for different modes of vibration were simulated using (19) (Figs. 4–7). The physical properties of the sensor element are shown in Table I. The simulation was carried out for two elastic body arrangements: one in which the elastic body covered the entire surface ( $x_1 = 0$  mm,  $x_2 = 7.5$  mm) and another in which it only covered the tip ( $x_1 = 6.5$  mm,  $x_2 = 7.5$  mm). The first mode was 3.8 kHz, the second mode was 24 kHz, the third mode was 66 kHz, and the fourth mode was 130 kHz. Figs. 4, 6, and 7 show that the changes in the output voltage induced by the changes in elasticity and viscosity are gradual when the mode of vibration is high. That is, the measurement range is narrow and the sensitivity is high when the mode of vibration is low, and the measurement range is wide and the sensitivity is low when the mode of vibration is high. Fig. 5 shows that when the elastic body is arranged so that it covers the entire surface, the change in the output voltage induced by the change in the viscosity does not depend on the mode of vibration and is constant. Figs. 4–7 show

$$z_n = \frac{bY_p d_{31} V (2t_s + t_p) Z_n \int_0^L Z_n [\delta(x) - \delta(x-L)] dx \cos(\omega_n t - \phi)}{2\sqrt{(bk_e A_x)^2 + \omega_n^2 (bc_e A_x + cA_L)^2}} \quad (12)$$

$$V_s = -\frac{b^2 Y_p^2 d_{31}^2 V (2t_s + t_p)^2 \int_0^L \frac{\partial^2 Z_n}{\partial x^2} dx \int_0^L Z_n [\delta(x) - \delta(x-L)] dx}{4C \sqrt{(bk_e A_x)^2 + \omega_n^2 (bc_e A_x + cA_L)^2}} \cos(\omega_n t - \phi) \quad (17)$$

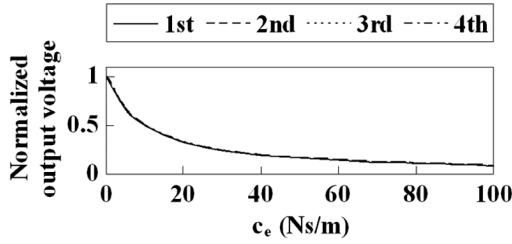


Fig. 5. Simulation results. Relationship between normalized output voltage and viscosity ( $x_1 = 0$  mm,  $x_2 = 7.5$  mm).

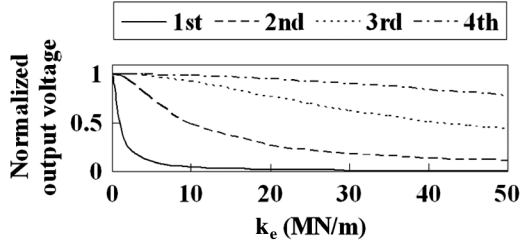


Fig. 6. Simulation results. Relationship between normalized output voltage and elasticity ( $x_1 = 6.5$  mm,  $x_2 = 7.5$  mm).

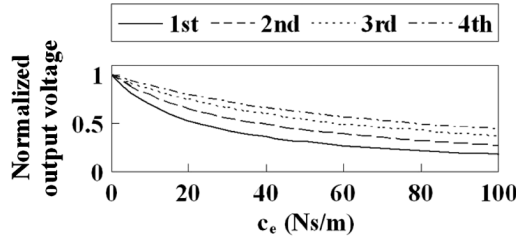


Fig. 7. Simulation results. Relationship between normalized output voltage and viscosity ( $x_1 = 6.5$  mm,  $x_2 = 7.5$  mm).

that when the elastic body is arranged so that it only covers the tip, the measurement range is wide and the sensitivity is low, compared with the case in which the elastic body is arranged so that it covers the entire surface. It should be noted that the measurement range does not widen in certain arrangements of the elastic body (for example,  $x_1 = 1$  mm and  $x_2 = 3$  mm), even when the mode of vibration is high.

To understand the change in sensitivity induced by the change in the mode of vibration in more detail, the gradients (sensitivity) of the curves shown in Figs. 4–7 are derived. From (19), the sensitivity is expressed as a function of the change in elasticity as

$$\begin{aligned} \text{Sensitivity}_{k_e} &\equiv -\frac{\partial V_1}{\partial k_e} \\ &= \frac{\omega_n c (b A_x)^2 k_e A_L}{[(b k_e A_x)^2 + \omega_n^2 (b c_e A_x + c A_L)^2]^{\frac{3}{2}}}. \end{aligned} \quad (20)$$

From (19), the sensitivity is expressed as a function of the change in viscosity as

$$\begin{aligned} \text{Sensitivity}_{c_e} &\equiv -\frac{\partial V_1}{\partial c_e} \\ &= \frac{\omega_n^3 b c (b c_e A_x + c A_L) A_x A_L}{[(b k_e A_x)^2 + \omega_n^2 (b c_e A_x + c A_L)^2]^{\frac{3}{2}}}. \end{aligned} \quad (21)$$

TABLE I  
PHYSICAL PROPERTIES OF SENSOR ELEMENT

Width	b	5	mm
Young's modulus of piezoelectric ceramics	$Y_p$	62	GPa
Piezoelectric constant	$d_{31}$	210	pm/V
Input voltage	V	10	$V_{p-p}$
Half thickness of substrate	$t_s$	25	$\mu\text{m}$
Thickness of piezoelectric ceramics	$t_p$	200	$\mu\text{m}$
Viscous damping coefficient	c	0.05	N-s/m
Young's modulus of substrate	$Y_s$	105	GPa
Density of substrate	$\rho_s$	4500	$\text{kg/m}^3$
Density of piezoelectric ceramics	$\rho_p$	7650	$\text{kg/m}^3$
Length	L	7.5	mm
Relative permittivity of piezoelectric ceramics	$\epsilon_p$	2130	
Capacitance	C	3.54	nF

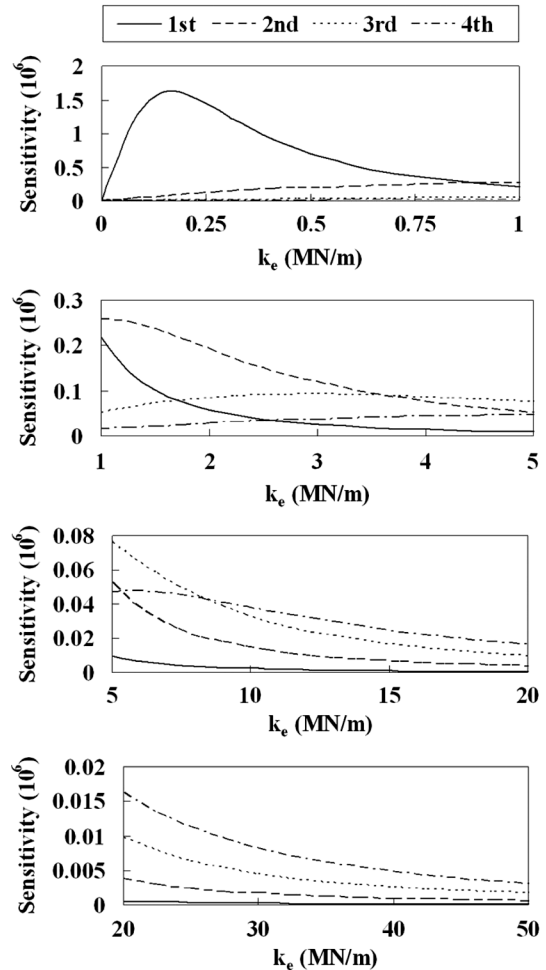


Fig. 8. Simulation results. Relationship between sensitivity and elasticity ( $x_1 = 0$  mm,  $x_2 = 7.5$  mm).

The sensitivities corresponding to the data plotted in Figs. 4–7 were derived using (20) and (21) (Figs. 8–11). Fig. 8 shows that the sensitivity of the first mode is the highest when  $k_e$  is 0–0.9 MN/m, the sensitivity of the second mode is highest when  $k_e$  is 0.9–3.6 MN/m, the sensitivity of the third mode

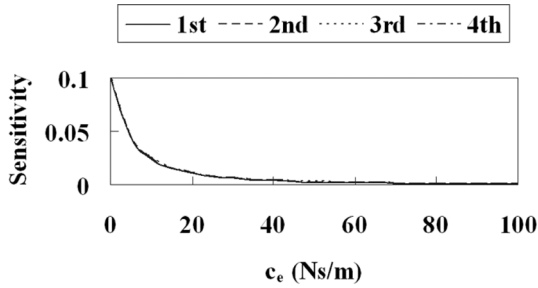


Fig. 9. Simulation results. Relationship between sensitivity and viscosity ( $x_1 = 0$  mm,  $x_2 = 7.5$  mm).

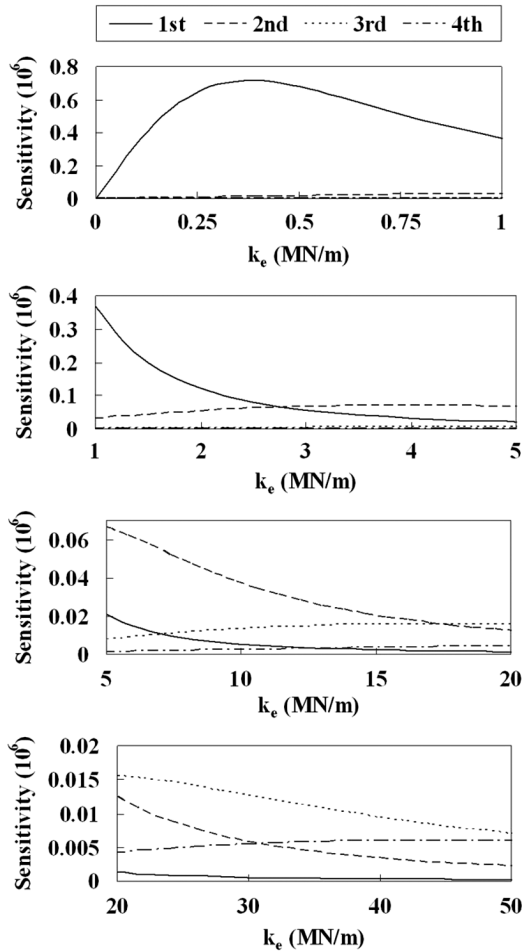


Fig. 10. Simulation results. Relationship between sensitivity and elasticity ( $x_1 = 6.5$  mm,  $x_2 = 7.5$  mm).

is highest when  $k_e$  is 3.6–8 MN/m, and the sensitivity of the fourth mode is highest when  $k_e$  is 8–50 MN/m. Fig. 10 shows that the sensitivity of the first mode is the highest when  $k_e$  is 0–2.8 MN/m, the sensitivity of the second mode is highest when  $k_e$  is 2.8–18 MN/m, and the sensitivity of the third mode is highest when  $k_e$  is 18–50 MN/m. Fig. 11 shows that the sensitivity of the first mode is the highest when  $c_e$  is 0–28 Ns/m, the sensitivity of the second mode is highest when  $c_e$  is 28–47 Ns/m, the sensitivity of the third mode is highest when  $c_e$  is 47–66 Ns/m, and the sensitivity of the fourth mode is highest when  $c_e$  is 66–100 Ns/m. From these results, it is clear that the lower the mode of vibration is, the higher the sensitivity

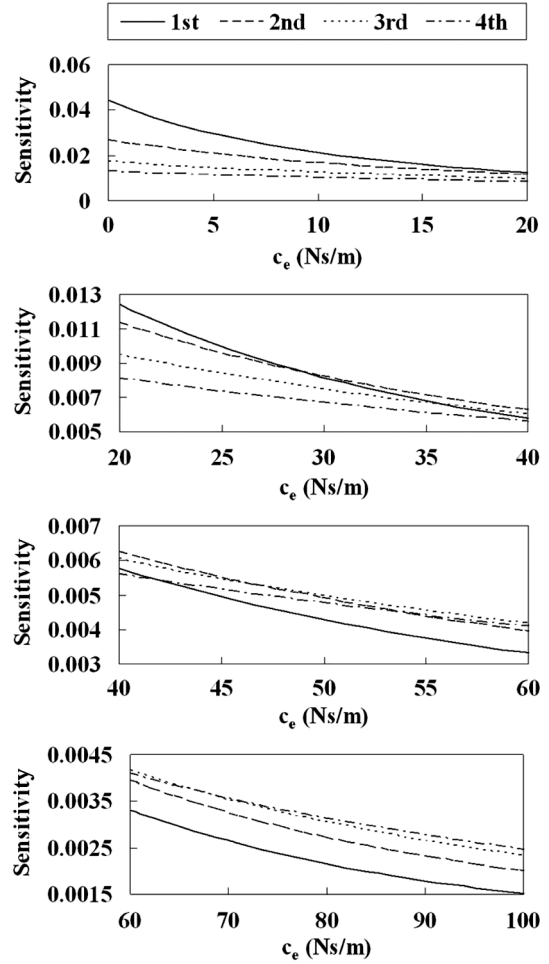


Fig. 11. Simulation results. Relationship between sensitivity and viscosity ( $x_1 = 6.5$  mm,  $x_2 = 7.5$  mm).

of the sensor to small changes in elasticity and viscosity is, and the higher the mode of vibration is, the lower the sensitivity of the sensor to large changes in elasticity and viscosity is.

### III. EXPERIMENT

To confirm the validity of the analytical results, a prototype was produced and evaluated. The prototype was produced by bonding two piezoelectric ceramic films (thickness = 200  $\mu$ m, width = 5 mm, PZT (C-6), Fuji Ceramics Corporation) to the upper and lower sides of a titanium substrate (thickness = 50  $\mu$ m, width = 5 mm) using conductive epoxy adhesive (Conductive Epoxy, Circuit Works Corporation) (Fig. 12). Table II shows the typical characteristics of the piezoelectric ceramics (the details of the characteristics are described in [18]). The evaluation system is shown in Fig. 13. The elastic body (urethane gel, thickness 5 mm, Exseal Corporation) covered with the silicon film (thickness = 50  $\mu$ m) is positioned between the prototype (length = 7.5 mm) and an electronic balance (BL-620S, Shimadzu Corporation). The prototype is moved downward, and the output voltage of the prototype and the pressure applied to the prototype are measured. The input voltage was 10  $V_{p-p}$ , and the experiment was carried out for two elastic body arrangements: one in which the elastic body covered the entire

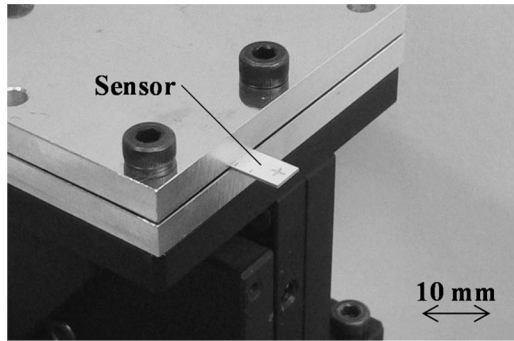


Fig. 12. Photograph of prototype. The size of the sensor element is about  $0.5 \times 5 \times 7.5$  mm.

TABLE II  
CHARACTERISTICS OF PIEZOELECTRIC CERAMICS

Young's modulus of piezoelectric ceramics	$Y_p$	62	GPa
Piezoelectric constant	$d_{31}$	210	pm/V
Density of piezoelectric ceramics	$\rho_p$	7650	kg/m <sup>3</sup>
Relative permittivity of piezoelectric ceramics	$\epsilon_p$	2130	

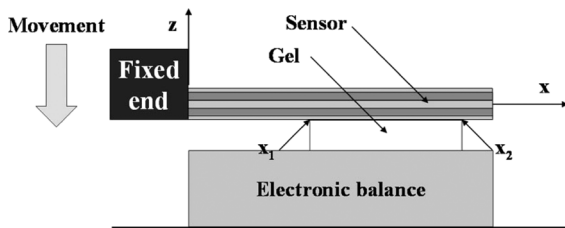


Fig. 13. Experimental system. The gel is positioned between the prototype and an electronic balance. The prototype is moved downward, and the output voltage of the prototype and the pressure applied to the prototype are measured.

surface ( $x_1 = 0$  mm,  $x_2 = 7.5$  mm) and another in which it only covered the tip ( $x_1 = 6.5$  mm,  $x_2 = 7.5$  mm), as in the analysis. The experimental results are shown in Figs. 14–17, and the normalized results calculated using (18) are shown in Figs. 18 and 19. Since the signal-to-noise ratio was small for the second mode and the fourth mode, they were not measured (in order to enlarge signal-to-noise ratio for these modes of vibrations, it is necessary to optimize the arrangement of the measurement electrode [13], [14]). Figs. 18 and 19 show that when the sensor element is driven in the first mode (3.5 kHz), the measurement range is narrow and the sensitivity is high, and when driven in the third mode (63 kHz), the measurement range is wide and the sensitivity is low. These results qualitatively correspond to the analytical results. Moreover, when the elastic body is arranged so as to not cover the entire surface (Fig. 18) but only the tip (Fig. 19), the measurement range is wide and the sensitivity is low. These results also qualitatively correspond to the analytical results. It is necessary to quantitatively derive the relationships between the applied force and the changes in elasticity and viscosity of the elastic body to allow quantitative comparison of the analytical results and the experiment results. It should be noted that Figs. 14 and 15 show that this tactile sensor can measure a pressure of 2.5 Pa and a pressure of 10 kPa by using two modes of vibration. Moreover, since a pressure of

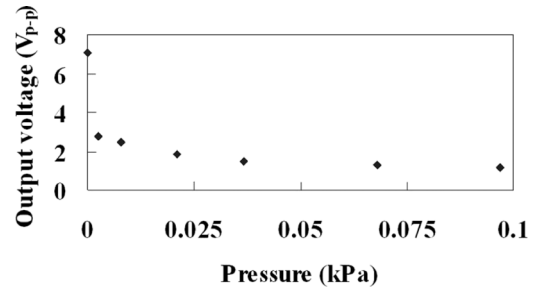


Fig. 14. Experimental results. Relationship between sensor output and pressure (first mode,  $x_1 = 0$  mm,  $x_2 = 7.5$  mm).

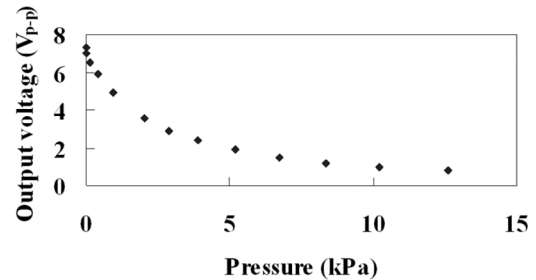


Fig. 15. Experimental results. Relationship between sensor output and pressure (third mode,  $x_1 = 0$  mm,  $x_2 = 7.5$  mm).

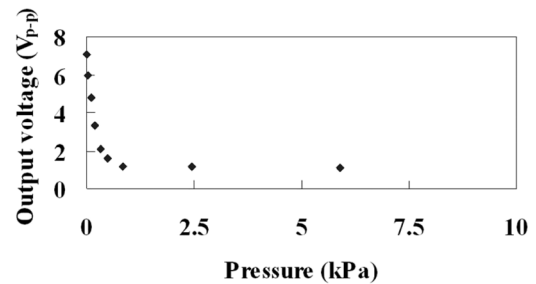


Fig. 16. Experimental results. Relationship between sensor output and pressure (first mode,  $x_1 = 6.5$  mm,  $x_2 = 7.5$  mm).

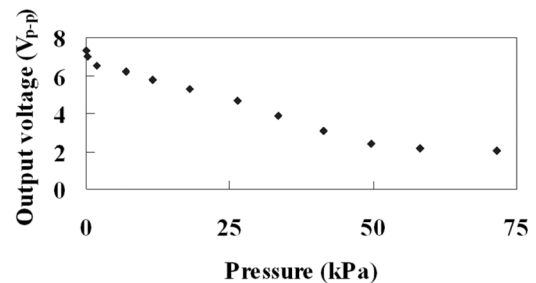


Fig. 17. Experimental results. Relationship between sensor output and pressure (third mode,  $x_1 = 6.5$  mm,  $x_2 = 7.5$  mm).

1 Pa can be measured from Fig. 14, the ratio between minimum and maximum measurement value is  $10^4$  or more.

#### IV. EVALUATION OF PRESSURE RESISTANCE

The pressure resistance was evaluated. The experimental system is shown in Fig. 20. The elastic body was placed on the sensor element fixed in the simply supported beam (length = 7.5 mm) with bonding tape, and the relationships

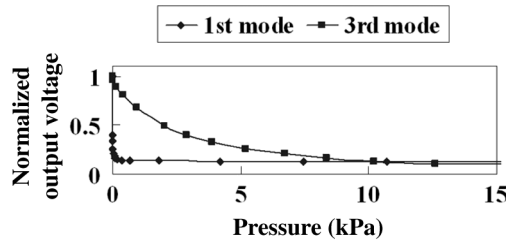


Fig. 18. Relationship between normalized sensor output and pressure ( $x_1 = 0$  mm,  $x_2 = 7.5$  mm).

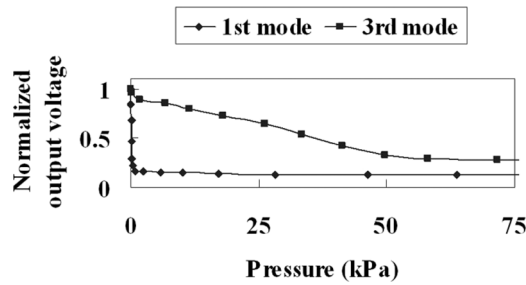


Fig. 19. Relationship between normalized sensor output and pressure ( $x_1 = 6.5$  mm,  $x_2 = 7.5$  mm).

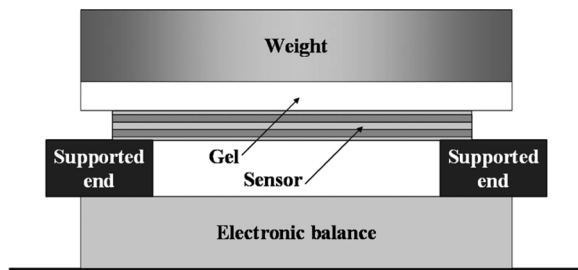


Fig. 20. Experimental system. The gel is placed on the sensor element fixed in the simply supported beam, and the relationships between the output voltage and pressure before and after the weight is applied are measured.

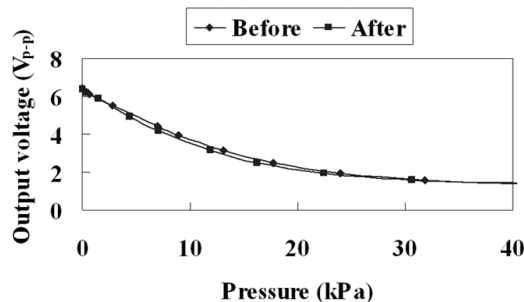


Fig. 21. Experimental results. Relationships between the output voltage and pressure before and after the weight was applied.

between the output voltage and pressure before and after the weight was applied were measured. A load of 10 kg (1.3 MPa) was applied because it was considered that this tactile sensor could be applied to a humanoid robot if the pressure resistance was 1 MPa or more. The input voltage was  $10 V_{p-p}$  (61 kHz). The experimental results are shown in Fig. 21. These results show that the characteristics of this tactile sensor negligibly changed after the load was applied. That is, this tactile sensor has a pressure resistance of at least 1 MPa or more. Moreover, this tactile sensor also showed reproducibility with application of an external force.

## V. CONCLUSION

In this paper, a new tactile sensor utilizing piezoelectric vibration was proposed. First, this tactile sensor was analyzed, and its characteristics were derived. The analytical results showed that the sensitivity of this tactile sensor changed with the mode of vibration of the sensor element and the arrangement of the elastic body with respect to the sensor element. These results qualitatively corresponded to the experiment results. Next, a prototype was produced and evaluated. The evaluation results showed that this tactile sensor can measure a pressure of 2.5 Pa and a pressure of 10 kPa and its pressure resistance is 1 MPa or more.

Since this tactile sensor has a high sensitivity, wide measurement range, pressure resistance, flexibility, and self-sensing function, it will be useful as a tactile sensor for a humanoid robot. In particular, since the ratio between minimum and maximum measurement value is  $10^4$  or more, various works can be executed like human hands. In future work, we will integrate this tactile sensor and apply it to artificial skin and a robotic hand.

## REFERENCES

- [1] J. G. da Silva, A. A. de Carvalho, and D. D. da Silva, "A strain gauge tactile sensor for finger-mounted applications," *IEEE Trans. Instrum. Meas.*, vol. 51, no. 1, pp. 18–22, Feb. 2002.
- [2] F. Castelli, "An integrated tactile-thermal robot sensor with capacitive tactile array," *IEEE Trans. Ind. Appl.*, vol. 38, no. 1, pp. 85–90, Jan.–Feb. 2002.
- [3] M. Shimojo, A. Namiki, M. Ishikawa, R. Makino, and K. Mabuchi, "A tactile sensor sheet using pressure conductive rubber with electrical-wires stitched method," *IEEE Sensors J.*, vol. 4, no. 5, pp. 589–596, Oct. 2004.
- [4] J. Dargahi, "An endoscopic and robotic tooth-like compliance and roughness tactile sensor," *J. Mech. Des.*, vol. 124, pp. 576–582, 2002.
- [5] [Online]. Available: [http://www.nitta.co.jp/english/product/mechasesen/sensor/tactile\\_top.html](http://www.nitta.co.jp/english/product/mechasesen/sensor/tactile_top.html)
- [6] H. Kawasaki, T. Komatsu, and K. Uchiyama, "Dexterous anthropomorphic robot hand with distributed tactile sensor: Gifu hand II," *IEEE/ASME Trans. Mechatronics*, vol. 7, pp. 296–303, 2002.
- [7] M. Ohka, Y. Mitsuya, Y. Matsunaga, and S. Takeuchi, "Sensing characteristics of an optical three-axis tactile sensor under combined loading," *Robotica*, vol. 22, pp. 213–221, 2004.
- [8] K. Kamiyama, H. Kajimoto, N. Kawakami, and S. Tachi, "Evaluation of a vision-based tactile sensor," in *Proc. IEEE Int. Conf. Robot. Autom.*, 2004, pp. 1542–1547.
- [9] M. H. Lee and H. R. Nicholls, "Review article tactile sensing for mechatronics—A state of the art survey," *Mechatronics*, vol. 9, pp. 1–31, 1999.
- [10] R. Tajima, S. Kagami, M. Inaba, and H. Inoue, "Development of soft and distributed tactile sensors and the application to a humanoid robot," *Adv. Robotics*, vol. 16, pp. 381–397, 2002.
- [11] L. Du, G. Kwon, F. Arai, T. Fukuda, K. Itoigawa, and Y. Tukahara, "Structure design of micro touch sensor array," *Sens. Actuators A*, vol. 107, pp. 7–13, 2003.
- [12] T. Itoh, T. Ohashi, and T. Suga, "Scanning force microscope using piezoelectric excitation and detection," *IEICE Trans. Electron.*, vol. E78-C, pp. 146–151, 1995.
- [13] K. Motoo, F. Arai, T. Fukuda, T. Katsuragi, and K. Itoigawa, "High sensitive touch sensor with piezoelectric thin film for pipetting works under microscope," *Sens. Actuators A*, vol. 126, pp. 1–6, 2006.
- [14] K. Motoo, F. Arai, T. Fukuda, M. Matsubara, K. Kikuta, T. Yamaguchi, and S. Hirano, "Touch sensor for micromanipulation with pipette using lead-free (K, Na)(Nb, Ta)  $O_3$  piezoelectric ceramics," *J. Appl. Phys.*, vol. 98, p. 094505, 2005.
- [15] T. Inoue and S. Hirai, "Elastic model of deformable fingertip for soft-fingered manipulation," *IEEE Trans. Robot.*, vol. 22, no. 6, pp. 1273–1279, Dec. 2006.
- [16] T. Ikeda, "Electroacoustical constants of asymmetric piezoelectric bimorph," (in [in Japanese]) *Jpn. J. Acoustical Soc.*, vol. 23, pp. 300–310, 1967.
- [17] T. Ikeda, *Fundamentals of Piezoelectricity*. Oxford, U.K.: Oxford Univ. Press, 1990.
- [18] [Online]. Available: <http://www.fujicera.co.jp/product/e/index.html>



**Kohei Motoo** graduated from Nagoya University, Nagoya, Japan, in 2002. He received the M.S. degree from Nagoya University in 2004. He is currently working towards the Ph.D. degree at the Department of Micro-Nano Systems Engineering, Nagoya University.

He is mainly engaging in the research fields of micro-nano robotics and its application to the micro-nano assembly and bio automation, micro-nano manipulation, micro-nano sensors, and micro-nano actuators.



**Fumihito Arai** graduated from the Science University of Tokyo, Japan, in 1986. He received the M.S. degree from the Science University of Tokyo, Tokyo, in 1988 and the Doctor of Engineering degree from Nagoya University, Nagoya, Japan, in 1993.

From 1988 to 1989, he was with Fuji Photo Film Company, Ltd., Japan. He joined Nagoya University in 1989. He is a Professor with the Department of Bioengineering and Robotics, Tohoku University. He is mainly engaging in the research fields of micro-nano robotics and its application to the micro-nano

assembly and bio automation, micro-nano manipulation, micro-nano sensors and micro-nano actuators, medical microsystems, intelligent robotic systems, and intelligent human machine interface.



**Toshio Fukuda** (M'83–SM'93–F'95) graduated from Waseda University, Tokyo, Japan, in 1971. He received the M.S. degree and the Doctor of Engineering degree from the University of Tokyo, Tokyo, Japan, in 1973 and 1977, respectively.

In 1977, he joined the National Mechanical Engineering Laboratory in Japan. He joined the Science University of Tokyo in 1981. He is a Professor with the Department of Micro-Nano Systems Engineering, Nagoya University, Nagoya, Japan. He is mainly engaging in the research fields of intelligent

robotic system, self-organizing system, micro-nano robotics, robotic system under hostile environment, bio-robotic system, neuromorphic intelligent control, fuzzy control, control of mechanical systems, and technical diagnosis.

Prof. Fukuda is a member of the Administrative Committees of the IEEE Robotics and Automation Society and the IEEE Industrial Electronics Society. He was the Vice President of the IEEE Industrial Electronics Society (1990), the Publication Chairman (1991–1992), the Secretary of the IEEE Neural Network Council (1992–1993), and was the President of the IEEE Robotics and Automation Society (1998–1999). He was elected as Director of the IEEE Division X, Systems and Control (2001–2002) and a founding President of the IEEE Nanotechnology Council (2002–2005).